Biological Psychiatry

Archival Report

Mapping Neurophysiological Subtypes of Major Depressive Disorder Using Normative Models of the Functional Connectome

Xiaoyi Sun, Jinrong Sun, Xiaowen Lu, Qiangli Dong, Liang Zhang, Wenxu Wang, Jin Liu, Qing Ma, Xiaoqin Wang, Dongtao Wei, Yuan Chen, Bangshan Liu, Chu-Chung Huang, Yanting Zheng, Yankun Wu, Taolin Chen, Yuqi Cheng, Xiufeng Xu, Qiyong Gong, Tianmei Si, Shijun Qiu, Ching-Po Lin, Jingliang Cheng, Yanqing Tang, Fei Wang, Jiang Qiu, Peng Xie, Lingjiang Li, Yong He, DIDA-MDD Working Group, and Mingrui Xia

ABSTRACT

BACKGROUND: Major depressive disorder (MDD) is a highly heterogeneous disorder that typically emerges in adolescence and can occur throughout adulthood. Studies aimed at quantitatively uncovering the heterogeneity of individual functional connectome abnormalities in MDD and identifying reproducibly distinct neurophysiological MDD subtypes across the lifespan, which could provide promising insights for precise diagnosis and treatment prediction, are still lacking.

METHODS: Leveraging resting-state functional magnetic resonance imaging data from 1148 patients with MDD and 1079 healthy control participants (ages 11–93), we conducted the largest multisite analysis to date for neurophysiological MDD subtyping. First, we characterized typical lifespan trajectories of functional connectivity strength based on the normative model and quantitatively mapped the heterogeneous individual deviations among patients with MDD. Then, we identified neurobiological MDD subtypes using an unsupervised clustering algorithm and evaluated intersite reproducibility. Finally, we validated the subtype differences in baseline clinical variables and longitudinal treatment predictive capacity.

RESULTS: Our findings indicated great intersubject heterogeneity in the spatial distribution and severity of functional connectome deviations among patients with MDD, which inspired the identification of 2 reproducible neurophysiological subtypes. Subtype 1 showed severe deviations, with positive deviations in the default mode, limbic, and subcortical areas and negative deviations in the sensorimotor and attention areas. Subtype 2 showed a moderate but converse deviation pattern. More importantly, subtype differences were observed in depressive item scores and the predictive ability of baseline deviations for antidepressant treatment outcomes.

CONCLUSIONS: These findings shed light on our understanding of different neurobiological mechanisms underlying the clinical heterogeneity of MDD and are essential for developing personalized treatments for this disorder.

https://doi.org/10.1016/j.biopsych.2023.05.021

Major depressive disorder (MDD) is one of the most prevalent and burdensome psychiatric disorders worldwide (1). It typically emerges in adolescence and can occur throughout adulthood and is accompanied by heterogeneous emotional, neurovegetative, and neurocognitive symptoms (2–4). This clinical diversity creates a huge challenge for disease diagnosis and treatment prediction. However, the underlying neurophysiological substrates of clinical heterogeneity remain largely unclear. Parsing neurophysiological heterogeneity is essential to better link complex biological dysregulations with clinical manifestations, thereby facilitating optimized treatment allocation for patients. Previous studies have attempted to identify MDD subtypes based on clinical symptoms, such as melancholic depression, atypical depression, and seasonal affective disorder (5–7). These studies have shown neurophysiological differences between the clinical subtypes and indicated a possible relationship between specific depressive symptom profiles and biological dysregulations. However, clinical symptoms interact in a complex manner with biological substrates and may change over age and disease course, and neurophysiologically informed subtyping of MDD is still lacking. Exploring neurophysiological MDD subtypes is expected to provide a more objective understanding of the biological mechanisms underlying the complex clinical heterogeneity and inspire imaging-derived candidate phenotypes for the guidance of future precise diagnostic methods and treatments.

Based on resting-state functional magnetic resonance imaging (rs-fMRI), many case-control studies have documented

SEE COMMENTARY ON PAGE e45

 ISSN: 0006-3223

disrupted functional brain connectomes in patients with MDD (8–11), thereby significantly enhancing our understanding of the neurophysiological substrates of this disease. Notably, the results from the between-group comparisons in small-sample studies were largely inconsistent, and the effect sizes were small in recent large-sample multisite studies. These observations recently led to an increased focus on the heterogeneity of functional connectomes among patients with MDD (12–14) and on the investigation of neurophysiological subtypes based on functional connectomes (15–19). Studies have found the important roles of functional connectomes of default mode network (DMN), limbic system (LIM), and subcortical (SUB) regions for MDD subtyping. For example, Liang *et al.* (17) found hyperconnectivity of DMN areas in one subtype and hypoconnectivity in the other subtype. Drysdale *et al.* (16) defined 4 neurophysiological subtypes based on the distinct functional connectivity patterns in LIM and frontostriatal networks. These studies observed differences in clinical presentations and treatment response among neurophysiological subtypes, which indicates the promise of discovering clinically valuable neurobiological subtypes based on functional connectomes. However, previous studies have largely ignored the fact that the functional connectomes can change dramatically over the lifespan and that individual abnormal measurements, quantitatively obtained from changes during a typical lifespan, can provide more accurate and disease-specific information for subtyping. Moreover, most previous studies lacked the reproducible validation of results from multiple centers. Reproducible neurophysiological subtypes hold promise for the future of personalized diagnosis and treatment of a more general population with MDD.

The normative model, a cutting-edge statistical framework that maps demographic or behavioral variables onto a neuroimaging feature, has demonstrated its superiority in characterizing the expected change trajectory of neuroimaging features in healthy control participants (HCs) and quantitatively identifying heterogeneous individual deviations for psychiatric disorders from the norm (20–22). Similar to the widely used normative growth charts used in pediatric medicine, where a child's height or weight is compared with the normative distribution for that particular age and sex (23), the normative model can be used to evaluate individuals in relation to a neuroimaging normative feature for a particular age and sex. Unlike the traditional case-control analysis, which provides information only on group-level abnormalities, the normative model considers intersubject differences within the patient and control groups and allows for measuring individual deviations from a typical trajectory (21,24–26). These individual deviations lead to a quantitative characterization of patients' developmental abnormalities and intersubject heterogeneity, which provides critical information for detecting neurobiological subtypes with distinct biological dysregulations and clinical manifestations (27).

In this study, we conducted a comprehensive investigation into the neurobiological heterogeneity and subtypes of MDD using a large, multisite rs-fMRI dataset of 2227 participants. We adopted a novel normative model framework, which allowed us to quantitatively estimate individual deviations in functional connectivity strength (FCS) over a lifespan. Through the analysis of these deviations, we aimed to uncover the intersubject heterogeneity among patients with MDD and identify reproducible neurobiological subtypes based on their deviation patterns. The identified neurobiological MDD subtypes were evaluated by testing for and examining multiple demographic and clinical variable differences among them.

METHODS AND MATERIALS

Imaging Dataset and Preprocessing

In this study, we used a strictly quality-controlled imaging dataset, including 1148 patients with MDD and 1079 matched HCs from 9 research centers from the DIDA-MDD (Disease Imaging Data Archiving - Major Depressive Disorder Working Group) (11) (Table 1; Figure S1). A subsample of 43 patients received a 6-month treatment with paroxetine, and treatment outcomes were recorded (Table S1). All rs-fMRI data of participants were obtained using 3T MRI scanners and then preprocessed using a standard pipeline as described in our previous work (11,28) (Table S2).

Normative Modeling for FCS

First, we computed the whole-brain FCS values for each participant based on a predefined functional parcellation (29), including 220 cerebral regions that had qualified fMRI signals in all participants (Supplement). Then, for each brain region, we estimated a normative model of FCS as a function of age and sex by using Gaussian process regression (20) in the HCs (Figure 1A; Supplement). Gaussian process regression is a Bayesian nonparametric interpolation method that yields coherent measures of predictive confidence alongside point estimates (30). In addition to fitting potentially nonlinear predictions of a brain feature, it can provide regional estimates of the expected variation in the relationship between age and brain features (normative variance) and estimates of uncertainty in this variance. To assess the generalizability of the models, we first estimated the normative models in the HCs under 10-fold cross-validation (Supplement), and overall standardized mean squared error and mean squared log-loss were used to evaluate the models. Then, the final normative models were trained on all HCs for the subsequent MDD deviation analyses. To evaluate potential age/sex effects on model design, we also constructed the normative models in young/old and female/male groups separately (Supplement).

Estimating Individual FCS Deviations in Normative Models for Patients With MDD

For each patient with MDD, the FCS of the brain regions were positioned on the normative percentile charts from HCs to estimate individual deviation (Figure 1B). We derived a z value that quantifies the deviation from the normative model in each brain region based on their observed FCS values and the predictive FCS values obtained from the model (Supplement) (20). The influence of patient sites on the calculation of FCS deviations was assessed in the validation analyses (Supplement). Similarly, the individual deviation map of each HC was estimated by computing the z values during 10-fold cross-validation. To further define the extreme individual-level deviations in the FCS of participants, we thresholded the deviation maps using $z = \pm 2.6$ (corresponding to a

Table 1. Demographic and Clinical Characteristics of the Participants

Center	Group	Age, Years, Mean (SD)	Sex, Female/ Male, *n*	Duration of Illness, Years, Mean (SD)	First Episode/ Recurrent Episode, *n*	Medicated, Yes/No, *n*	HDRS-17, Mean (SD)	Age at Illness Onset, Years, Mean (SD)	Mean FD, mm, Mean (SD)
CMU, Shenyang	Patients, *n* = 125	27.91 (9.70)	86/39	1.65 (3.17)	100/11	49/76	21.44 (8.67)	26.36 (9.93)	0.115 (0.072)
	HCs, *n* = 248	27.25 (8.22)	145/103						0.107 (0.057)
	t or χ^2, *p*	$t_{371} = 0.69$, $p = .493$	$\chi_1^2 = 3.76$, $p = .052$						$t_{371} = 1.09$, $p = .278$
CSU, Changsha	Patients, *n* = 177	36.28 (10.21)	100/77	2.83 (3.95)	NA	NA	23.24 (5.91)	30.97 (8.43)	0.141 (0.073)
	HCs, *n* = 108	32.31 (7.96)	46/62						0.134 (0.064)
	t or χ^2, *p*	$t_{283} = 3.45$, $p = .001$	$\chi_1^2 = 5.19$, $p = .023$						$t_{283} = 0.90$, $p = .371$
GCMU1, Guangzhou	Patients, *n* = 34	29.41 (8.27)	25/9	0.65 (0.70)	34/0	0/34	21.85 (2.25)	NA	0.094 (0.030)
	HCs, *n* = 34	30.09 (10.88)	24/10						0.096 (0.033)
	t or χ^2, *p*	$t_{66} = -0.29$, $p = .774$	$\chi_1^2 = 0.07$, $p = .787$						$t_{66} = -0.26$, $p = .797$
GCMU2, Guangzhou	Patients, *n* = 66	29.48 (9.91)	41/25	0.76 (1.00)	66/0	0/66	22.30 (3.57)	NA	0.089 (0.057)
	HCs, *n* = 66	29.33 (10.12)	35/31						0.086 (0.042)
	t or χ^2, *p*	$t_{130} = 0.29$, $p = .774$	$\chi_1^2 = 1.12$, $p = .291$						$t_{130} = 0.29$, $p = .770$
KMU, Kunming	Patients, *n* = 41	34.20 (9.37)	21/20	1.13 (1.28)	NA	NA	23.61 (4.64)	NA	0.186 (0.083)
	HCs, *n* = 46	39.02 (12.20)	20/26						0.166 (0.065)
	t or χ^2, *p*	$t_{85} = -2.05$, $p = .043$	$\chi_1^2 = 0.52$, $p = .470$						$t_{85} = 1.25$, $p = .216$
PKU, Beijing	Patients, *n* = 75	31.51 (7.86)	31/44	0.52 (0.47)	75/0	0/75	25.35 (4.77)	30.99 (7.91)	0.175 (0.063)
	HCs, *n* = 73	31.90 (9.01)	31/42						0.185 (0.067)
	t or χ^2, *p*	$t_{146} = -0.29$, $p = .775$	$\chi_1^2 = 0.02$, $p = .889$						$t_{146} = -0.91$, $p = .362$
SCU, Chengdu	Patients, *n* = 48	35.75 (12.22)	25/23	1.13 (1.49)	28/19	23/25	22.88 (4.25)	35.17 (12.65)	0.111 (0.067)
	HCs, *n* = 41	34.83 (17.69)	24/17						0.122 (0.072)
	t or χ^2, *p*	$t_{87} = 0.29$, $p = .773$	$\chi_1^2 = 0.37$, $p = .542$						$t_{87} = -0.72$, $p = .473$
SWU, Chongqing	Patients, *n* = 282	38.74 (13.65)	183/99	4.20 (5.52)	209/49	124/125	20.94 (5.60)	NA	0.125 (0.054)
	HCs, *n* = 254	39.65 (15.80)	166/88						0.134 (0.063)
	t or χ^2, *p*	$t_{534} = -0.72$, $p = .472$	$\chi_1^2 = 0.01$, $p = .911$						$t_{534} = -1.68$, $p = .094$
YMU, Taipei	Patients, *n* = 105	57.05 (16.21)	42/63	1.21 (1.54)	NA	79/26	11.23 (6.46)	43.08 (15.30)	0.139 (0.082)
	HCs, *n* = 109	51.12 (11.70)	40/69						0.128 (0.058)
	t or χ^2, *p*	$t_{212} = 3.06$, $p = .003$	$\chi_1^2 = 0.25$, $p = .619$						$t_{212} = 1.18$, $p = .240$
ZZU, Zhengzhou	Patients, *n* = 195	18.40 (5.54)	98/97	1.29 (1.48)	NA	0/195	22.43 (5.70)	NA	0.100 (0.045)
	HCs, *n* = 100	22.43 (4.49)	53/47						0.088 (0.039)
	t or χ^2, *p*	$t_{293} = -6.29$, $p = <.001$	$\chi_1^2 = 0.20$, $p = .655$						$t_{293} = 2.16$, $p = .032$

Table 1. Continued

Center	Group	Age, Years, Mean (SD)	Sex, Female/Male, *n*	Duration of Illness, Years, Mean (SD)	First Episode/Recurrent Episode, *n*	Medicated, Yes/No, *n*	HDRS-17, Mean (SD)	Age at Illness Onset, Years, Mean (SD)	Mean FD, mm, Mean (SD)
All Data	Patients, *n* = 1148	33.83 (14.97)	673/475	2.10 (3.60)	512/79	277/622	21.31 (6.77)	32.74 (12.37)	0.125 (0.067)
	HCs, *n* = 1079	33.96 (13.87)	613/466						0.123 (0.063)
	t or χ^2, *p*	$t_{2225} = -0.21$, $p = .832$	$\chi_1^2 = 0.75$, $p = .387$						$t_{2225} = 0.80$, $p = .423$

The GCMU1 and GCMU2 datasets were collected using the same scanner at one site with different scan parameters.

CMU, China Medical University; CSU, Central South University; FD, framewise displacement; GCMU, Guangzhou University of Chinese Medicine; HC, healthy control participant; HDRS, Hamilton Depression Rating Scale; KMU, Kunming Medical University; NA, not available; PKU, Peking University; SCU, Sichuan University; SWU, Southwest University; YMU, National Yang-Ming University; ZZU, Zhengzhou University.

$p < .005$) as was done in previous studies (25,26,31). The effect on the results of different thresholds for defining extreme individual deviations was validated (Supplement). The overall deviations of each participant and the spatial overlap map of extreme deviations across participants were calculated to assess the intersubject heterogeneity. The between-group differences in the mean deviation map and the overall deviation indices between patients with MDD and HCs were compared using two-sample *t* tests. The significance level was corrected for multiple comparisons using the false discovery rate (FDR) method (corrected $q < .05$).

Characterizing MDD Subtypes Based on Individual FCS Deviations

We used a data-driven k-means clustering algorithm to explore MDD subtypes with different deviation patterns (Figure 1C; Supplement). The intersite reproducibility of subtyping was evaluated by comparing the number of patients within each subtype among different sites and repeating the clustering analysis based on leave-one-site-out validation (Supplement). For the obtained subtypes, the brain deviations and the demographic and clinical variables were further compared (Supplement). Support vector regression analysis was conducted to examine the predictive ability of baseline deviation values for treatment response in each patient subtype (Supplement).

RESULTS

Normative Models of FCS

The 10-fold cross-validation in the HCs revealed a high generalizability of the fitting performance of normative models for FCS, as indicated by an overall standardized mean squared error close to 1 (0.996 ± 0.013) and a mean squared log-loss close to 0 (-0.001 ± 0.007) (Figure S2). The normative models established in all HCs showed that the brain regions can be clustered (Supplement) into 2 categories according to their age-related FCS change trajectories in both female (Figure 2A) and male (Figure S3) groups. Specifically, regions with increased age-related FCS values were located mostly in the lateral frontoparietal cortices, dorsal anterior cingulate cortex, medial occipital cortices, sensorimotor areas, and subcortical areas, while those with decreased FCS were mainly in the precuneus, posterior cingulate cortex, medial prefrontal cortex, angular gyrus, insula, and medial temporal areas.

Highly Heterogeneous Individual Deviations From Normative Models in Patients With MDD

Compared with the HCs, patients with MDD exhibited larger individual FCS deviations, including the number of extremely deviated regions (Cohen's $d = 0.18$) and the sum of positive ($d = 0.17$) and negative ($d = -0.12$) extreme deviations (Figure 2B) (FDR-corrected $q < .05$). Regionally, the patient group had larger deviations than the HC group, with positive deviations mainly in the bilateral lateral frontal cortex, precuneus, angular gyrus, and subcortical areas and negative deviations in the left parahippocampal gyrus, right Rolandic operculum, and middle cingulum gyrus (Figure S4; Table S3) (absolute $d = 0.12$–0.21, FDR-corrected $q < .05$). A total of

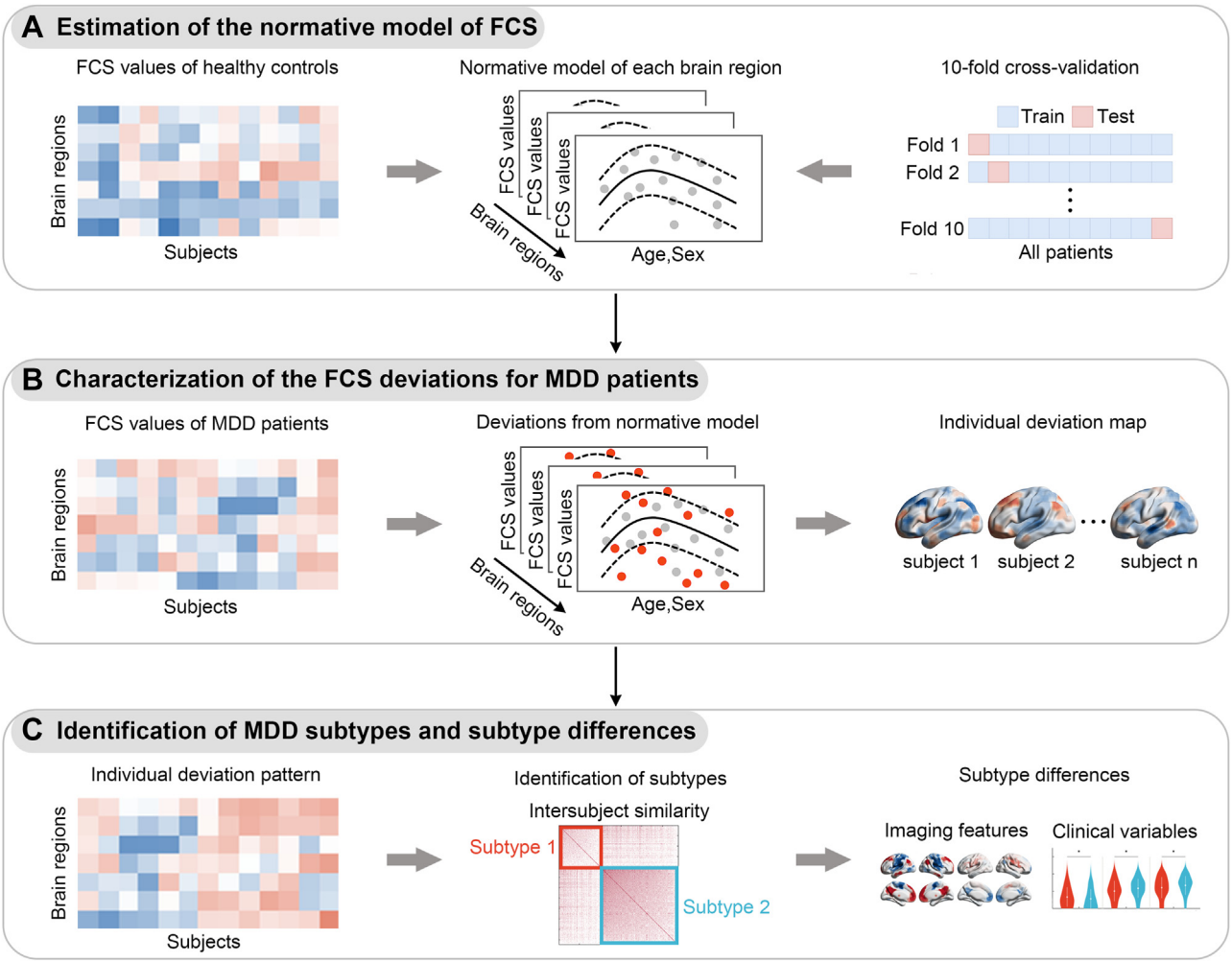

Figure 1. Flowchart of data analysis. **(A)** Estimation of the normative model of functional connectivity strength (FCS) for each brain region by training Gaussian process regression on the healthy control participant dataset (gray dots). The solid line represents the predicted FCS values from the normative model, and the dashed line indicates the normative range. Tenfold cross-validation was performed to assess the generalizability of the models. **(B)** Characterization of the FCS deviation of each brain region for each patient with major depressive disorder (MDD) (red dots) based on the normative model. **(C)** Identification of MDD subtypes based on the individual FCS deviation patterns and characterization of their imaging and clinical differences.

72.82% (n = 836) of the patients with MDD showed extreme FCS deviations from the normative model in at least one brain region, including extreme positive deviations in 25.78% (n = 296) of patients and extreme negative deviations in 66.38% (n = 762) of patients (Figure 2C). From the perspective of brain regions, 99.55% (n = 219) of the nodes showed an extreme FCS deviation in at least one patient (positive: 67.73%, n = 149; negative: 96.36%, n = 212). The extreme positive deviations in patients with MDD were mostly located in the prefrontal cortex, precuneus, angular gyrus, and subcortical areas, and the extreme negative deviations were widespread over the whole brain, especially in the medial sensorimotor cortex and the temporal lobe (Figure 2D). However, for any single brain region, the percentage of patients who deviated extremely from the normative range was remarkably low for both positive (≤2.35%, n = 27) and negative (≤3.14%, n = 36) deviations (Figure 2D). These findings suggest that while alterations in FCS existed in most patients with MDD, the specific brain regions having out-of-range alterations varied remarkably among individual patients.

FCS Deviation–Based MDD Subtypes

Two MDD subtypes were identified based on individual FCS deviations. This optimal subcluster number was consistently selected by 11 of 22 effective quality indices (Figure 3A). This subtyping result showed high intersite reproducibility, indicated by no significant site difference in the number of patients within each subtype (χ_9^2 = 14.74, p = .098), and the overlap rates of the resulting clustered indices in the leave-one-site-out validation with the clustered indices in the main results were all >92% (Figure 3B; Table S4).

Subtype 1 (37%, n = 425) showed severe deviations, with positive deviations in the DMN, LIM, and SUB areas

and negative deviations in the sensorimotor, dorsal attention, and ventral attention areas, while subtype 2 (63%, n = 723) showed moderate deviations with a conversed deviation pattern (Figure 3C; Table S5) (absolute d = 0.32–1.65, FDR-corrected $q < .05$). Statistical comparisons showed that all 3 overall deviation indices of subtype 1 were higher than those of HCs, while the number of extremely deviated regions and the sum of negative extreme deviations of subtype 2 were lower than those of HCs (Figure 3D; Table S6) (η_p^2 = 0.05–0.08, FDR-corrected $q < .05$). From the spatial overlap maps of extreme deviations, we observed a higher consistency of extremely deviated regions among patients with the severe-deviation subtype (positive: 0.23%–4.71%, d = 0.32; negative: 0.23%–5.88%, d = 0.35; FDR-corrected $q < .05$) and a lower consistency among patients with the moderate-deviation subtype (positive: 0.13%–2.49%, d = −0.31; negative: 0.13%–1.80%, d = −0.36; FDR-corrected $q < .05$) compared with that among all patients (Figure 3E).

Regarding demographic and clinical variables, severe-deviation subtype patients were significantly older on average (d = 0.16, p = .008) and had a higher medicated proportion (Cramer's V = 0.08, p = .013) than moderate-deviation subtype patients (Figure 4A; Table S7). The severe-deviation subtype had more severe symptoms as measured using the suicide item (d = 0.19, p = .044), while the moderate-deviation subtype exhibited more severe symptoms as measured by the work and activities (d = 0.29, p = .002) and depressed mood (d = 0.23, p = .016) items (Figure 4A; Table S7). Moreover, analysis of covariance showed that the correlations between the Hamilton Depression Rating Scale-17 item (HDRS-17) score and the onset age were significantly different between the 2 subtypes (η_p^2 = 0.01, p = .036) (Tables S8 and S9). The HDRS-17 score was negatively correlated with onset age in the severe-deviation subtype (r = −0.24, p = .004) but not in the moderate-deviation subtype (r = −0.00, p = .966) (Figure 4B). These neuroimaging and clinical differences between subtypes were largely unchanged under leave-one-site-out validation (Figure S5; Table S10).

Among the patients who had follow-up treatment outcomes (16 severe-deviation subtype patients and 27 moderate-deviation subtype patients), the baseline individual deviation map could significantly predict HDRS score changes after treatment for the severe-deviation subtype (r = 0.47, p = .019, one-tailed permutation test) (Figure 4C). The most positively contributive features were in the DMN (24.1%), frontoparietal network (16.1%), and ventral attention network (15.6%), and the most negatively contributive features were in the visual network (40.5%) (Figure 4C). In contrast, the baseline deviation map of the moderate-deviation subtype could not predict their HDRS score changes (r = −0.14, p = .785, one-tailed permutation test).

Validation Results

Overall, the findings reported above were generally reproducible across different analytical choices (Supplement). Under different thresholds in FCS calculation (r = 0.15, 0.25), in extreme deviation definition (FDR-corrected $q < .05$), and in constructing normative models in each age/sex subgroup, the normative models and patients' deviations were similar to our main results: the overlap rates of the resulting subtype indices with the clustered indices in the main results were >92% (range: 92.84%–99.22%), and the subtype differences largely remained (Figures S6–S13). There were no significant site-related effects in the deviation values of any of the brain regions (FDR-corrected q = .183∼.100).

DISCUSSION

In this study, we quantitatively uncovered neurophysiological heterogeneity and identified intersite reproducible MDD subtypes by mapping deviations from the normative models of functional connectome based on the currently largest rs-fMRI dataset in MDD. Our findings highlight the significant inter-subject variability in the spatial distribution and severity of functional connectome abnormalities among patients with MDD and accordingly suggest 2 neurobiological subtypes with distinct functional abnormality patterns and clinical characteristics. Our study offers a novel analytical framework for subtyping MDD and offers promising implications for future personalized diagnosis and treatment of this disorder.

Normative Models of FCS

Compared with the traditional general linear model, the normative model allows nonlinear changes to be characterized without assumptions about the change trajectories (24–27). Here, based on a large-sample dataset, we estimated the normative model of FCS for each brain region and found 2 categories of FCS change trajectories. Similar to our findings, several previous studies found linear age-related FCS decreases in the medial prefrontal cortex, precuneus, and insula and calcarine, and linear increases in sensorimotor areas based on the general linear model (32–34). The areas of FCS decrease are the prominent hubs of global and local functional connectivity, and the age-related decrease could underlie the performance decline in working memory and visual sustained attention, which are the most-affected cognitive functions that occur with aging (35–37). Conversely, the sensorimotor areas are the least affected by aging (32). Notably, in our study, although brain regions had overall increased or decreased change trajectories, the changes did not always follow a linear or quadratic change, which demonstrates the value of the normative model in characterizing the natural FCS change trajectories more accurately.

Highly Heterogeneous Individual Deviations From Normative Models in Patients With MDD

The normative model has shown its advantages in accurately quantifying patients' individual deviations from a large reference cohort by recognizing all sources of variance and reducing overly optimistic inferences (21,38). By exploring mechanisms and identifying potential subtypes of patients based on individual objective biological measures rather than their clinical diagnoses, the normative model provides a valuable framework to consider the challenging issues of comorbidity and heterogeneity in studies investigating neurophysiological mechanisms of mental disorders (38,39). Based on the normative model of FCS, we identified the

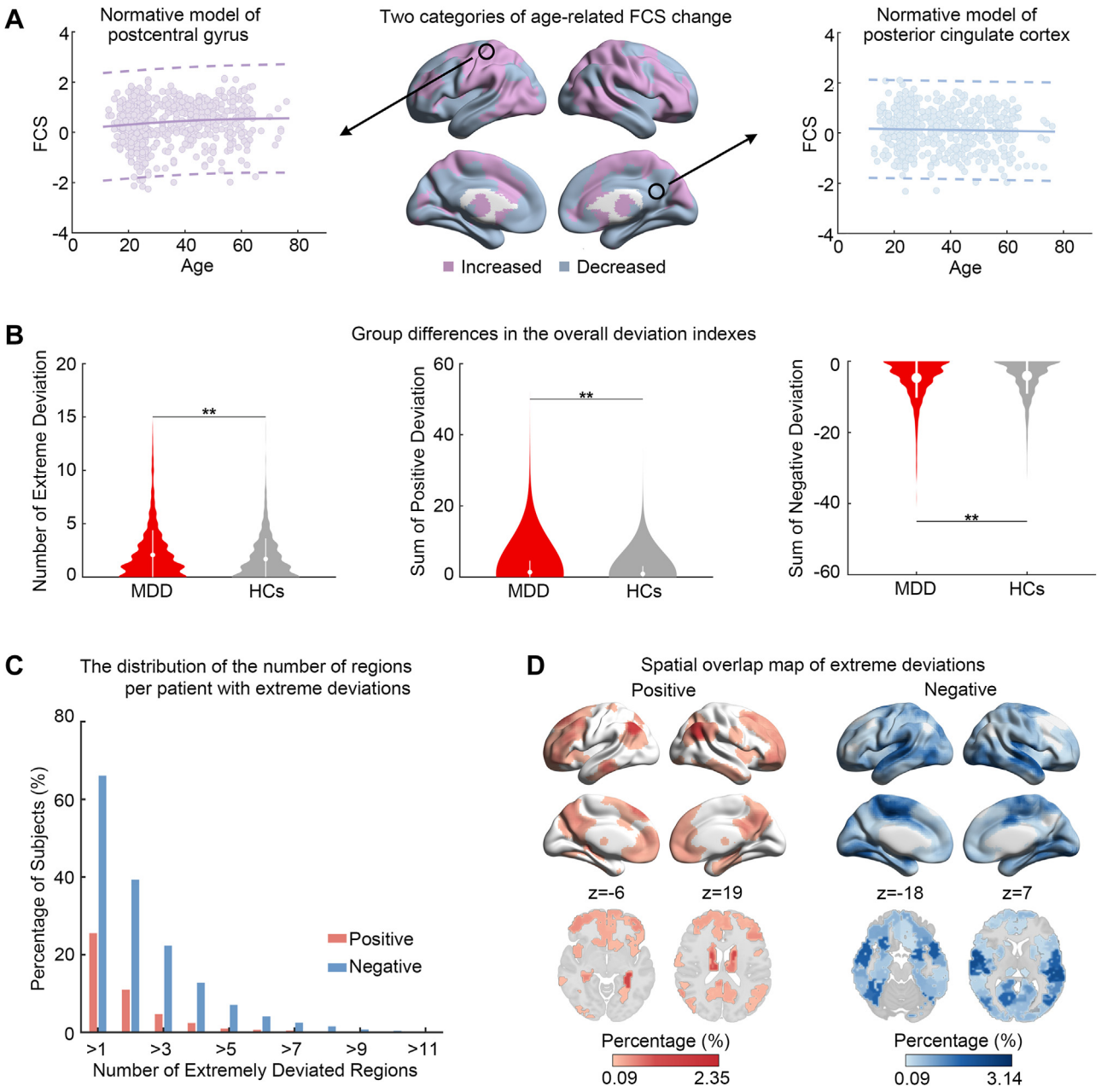

Figure 2. Normative models established in healthy control participants (HCs) and individual deviations from normative models in patients with major depressive disorder (MDD). **(A)** The brain map in the middle indicates the 2 categories of age-related functional connectivity strength (FCS) change trajectories (purple: increased; blue: decreased) in HCs (female). The FCS change trajectories (solid line) and the normative range (dashed line) of the postcentral gyrus and posterior cingulate cortex are shown on the left and right as examples. Each dot represents the data from 1 HC. **(B)** The between-group differences in the overall deviation indices between patients with MDD and HCs. **False discovery rate–corrected $q < .05$. **(C)** Bar plots show the distribution of the number of regions per patient with extremely positive (red) and negative (blue) deviations. **(D)** The spatial overlap maps indicate the percentage of patients who deviated extremely from the normative range for each brain region (left, extreme positive deviations; right, extreme negative deviations).

individual deviations for each patient with MDD and explored the heterogeneity of FCS deviations among patients. We found positive FCS deviations mainly in the DMN and SUB areas and negative deviations mainly in the sensorimotor and lateral temporal cortices. The increased FCS in the DMN and SUB indicates their strengthened role in coordinating whole-brain networks, which has been shown to be associated with internally directed cognitive rumination and emotional processing in patients with MDD (40,41). The decreased FCS in the sensorimotor and lateral temporal cortices suggests weakened integration of these regions, possibly reflecting impairments in decoding and integrating primary sensory input processing in

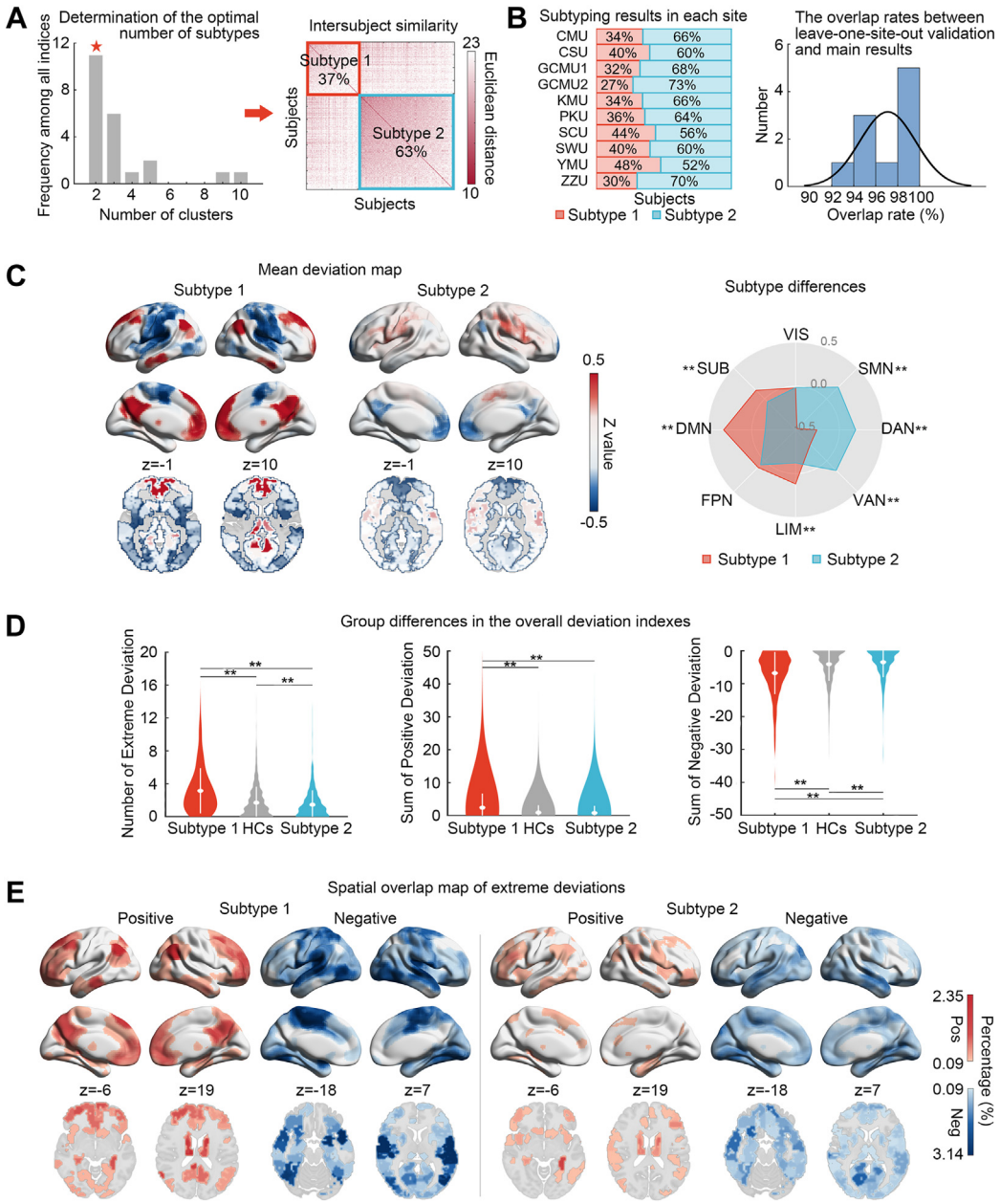

Figure 3. Functional connectivity strength (FCS) deviation–based major depressive disorder (MDD) subtypes. **(A)** Determination of the optimal number of MDD subtypes using the NbClust package and the intersubject similarity in the FCS deviation patterns among all patients. **(B)** Subtyping results in each site and the overlap rates of the resulting clustered indices in the leave-one-site-out validation with the clustered indices in the main results. **(C)** The mean deviation map of each subtype and their system-level differences. **(D)** The group differences in the overall deviation indices among MDD subtypes and healthy controls (HCs). **(E)** The spatial overlap map of extreme positive and negative deviations of each subtype. **False discovery rate–corrected $q < .05$. CMU, China Medical University; CSU, Central South University; DAN, dorsal attention network; DMN, default mode network; FPN, frontoparietal network; GCMU, Guangzhou University of Chinese Medicine; KMU, Kunming Medical University; LIM, limbic network; Neg, negative; PKU, Peking University; Pos, positive; SCU, Sichuan University; SMN, sensorimotor network; SUB, subcortical regions; SWU, Southwest University; VAN, ventral attention network; VIS, visual network; YMU, National Yang-Ming University; ZZU, Zhengzhou University.

patients (40,41). More importantly, we found that the overlap rates among patients in these regions were very low. This large interpatient heterogeneity provides an important cue to help explain the inconsistent findings in previous functional connectome studies in MDD. For example, the medial prefrontal cortex, which showed heterogeneous FCS alterations in our study, was found to have both increased and decreased FCS in previous case-control studies (41–44). Our results

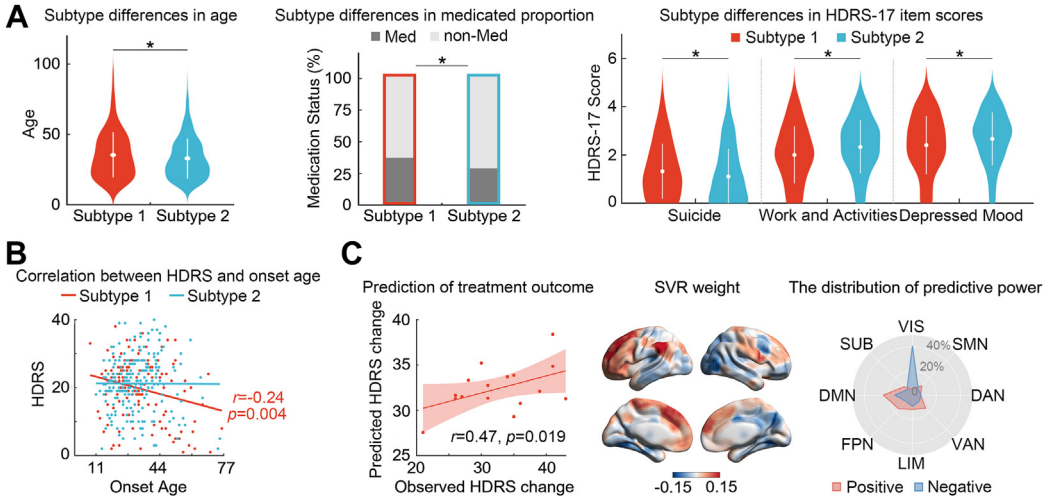

Figure 4. Subtype differences in demographic and clinical variables. **(A)** Subtype differences in age, medicated proportion, and Hamilton Depression Rating Scale-17 item (HDRS-17) score. *$p < .05$. **(B)** The correlation between the HDRS-17 total score and the onset age in each subtype. Each dot represents the data from 1 patient. **(C)** The predictive ability of deviation values for treatment response in patients of the severe-deviation subtype. The scatterplot presents the correlation between the observed HDRS score change after treatment and the predicted HDRS score change derived from the support vector regression (SVR). Each dot represents the data from 1 patient, and the dashes indicate the 95% prediction error bounds. The summed weights in 5-fold cross-validation were mapped onto the brain surface. The radar map represents the distribution of predictive power in different systems (red: positive; blue: negative). DAN, dorsal attention network; DMN, default mode network; FPN, frontoparietal network; LIM, limbic network; SMN, sensorimotor network; SUB, subcortical regions; VAN, ventral attention network; VIS, visual network.

suggest that FCS alteration is an important neuropathological feature of MDD, while the alteration patterns among patients are largely different and there may be multiple forms of MDD.

FCS Deviation–Based MDD Subtypes

We identified 2 subtypes; the severe-deviation subtype showed positive deviations in the DMN, LIM, and SUB areas, whereas in the moderate-deviation subtype the deviations of these regions were negative. These findings are consistent with several previous reports. For example, based on the power envelope–based connectivity of signals reconstructed from high-density resting-state electroencephalography, Zhang *et al.* (45) identified 2 MDD subtypes with different functional connectivity patterns of the frontoparietal-control network and DMN. Two other rs-fMRI studies also identified 2 subtypes with distinct functional connectivity patterns among DMN areas in patients with MDD (17,46). A transdiagnostic study, based on the whole-brain amplitude of low-frequency fluctuations, clustered patients with MDD into 2 subtypes with distinct activity patterns (47). Based on multimodal imaging data and different measures, these findings indicate that the functional connectome and activity of DMN areas are the most important biomarkers for the neurophysiological subtyping of MDD. Our study extends this understanding of neurophysiological MDD subtypes based on individual functional connectome abnormalities of patients against a reproducible normative trajectory derived from a large multisite cohort. Future studies combining different measures from multimodal imaging features may be helpful for better understanding disease heterogeneity and identifying patient-specific biomarkers for precise diagnosis and treatment of MDD. Notably, the current dataset was collected in China, and so it may be more representative of the Asian population. Although our subtyping results are consistent with the above-mentioned studies conducted in the Western population (45,46), it would be valuable to expand our sample to other ethnic groups through international collaborations to assess the generalizability of subtyping across different ethnicities (48,49).

We found that the severe-deviation subtype had a higher suicide item score on the HDRS-17. Previous studies have shown that the increased functional connectomes and activities of the DMN, LIM, and SUB areas, including the orbitofrontal cortex, medial prefrontal cortex, cingulate cortex, and striatum, are associated with suicide (50–53). More specifically, the orbitofrontal cortex is involved in learning, prediction, and decision making for emotional and reward-related behaviors and is important in regulating behavioral impulsivity and response inhibition (54). The higher FCS in the orbitofrontal cortex may be associated with increased vulnerability to suicidal behavior. Regions of the DMN are associated with self-referential processing. Evidence suggests that when individuals are involved in regurgitating negative emotions about themselves, suicidal thoughts and behaviors occur in response to the individual's desire to escape from both self-awareness and the associated unpleasant feelings (53,55). On the other hand, the moderate-deviation subtype showed more severe symptoms in the work and activities item and the depressed mood item, which are considered the core symptoms of patients with MDD in clinical diagnostics (56). The decreased functional connectomes in areas of the DMN, LIM, and SUB are considered to be related to anhedonia (57–63), which is defined as diminished interest or pleasure in response to stimuli that were previously perceived as rewarding in a premorbid state (58). Our results provide new evidence that the lower FCS in these areas is related to the nonreactive mood and the failure to respond to contextual changes in patients

with MDD. Additionally, a significant negative correlation between age of onset and HDRS-17 score was found only in the severe-deviation subtype. Several studies have explored the association between age of onset and HDRS-17 scores in patients with MDD, but the results have been inconsistent (64–67). Our results indicated that these inconsistent observations may be partly due to patient subtypes with different neurobiological mechanisms. More importantly, we found that the predictive power of FCS deviation patterns for treatment effects was observed only in the severe-deviation subtype, and the most contributing features were found in the DMN and visual network. Interestingly, previous studies have reported differential functional connectivity and activities of the DMN and visual network areas between treatment-resistant and treatment-sensitive patients, suggesting the potential predictive power of these areas for clinical outcomes in patients with MDD (11,68–70). Our findings extend this knowledge, demonstrating that this brain-phenotype relationship may exist in only one subtype of patients with severe brain alterations. Additionally, there is evidence that the recovery of elevated DMN FCS was significantly correlated with treatment response (43), while decreased DMN FCS was associated with nonresponse to first-line antidepressants (17). Combined with the subtype differences in depressive item scores, our study highlights the different mechanisms that underly the different clinical profiles and treatment responses among patients.

Limitations and Future Directions

Several issues with the current study need to be addressed further. First, our analysis was performed based on data from a cross-sectional sample, and the nonlinear age effects on characterizing trajectories and patient subtyping should be considered. Our validation analysis of constructing normative models in age/sex subgroup suggests that neurophysiological subtypes were not driven by age/sex effects, although there was a significant age difference between the 2 subtypes. Using longitudinal samples will improve the representativeness and accuracy of the age-related brain change curve by delineating the trajectories of each participant. Second, in this study, we compared the subtype differences in clinical symptoms using HDRS-17 item scores. The patients with MDD also had varied cognitive impairments, which were not assessed in the current retrospective study. Further analysis combined with more detailed cognitive performances could help us to better understand the complex relationship between the neurophysiological basis and the clinical presentations of MDD. Third, all the patients who were included in the analysis to predict treatment outcomes were responders to paroxetine because patients who had a poor response discontinued the medication or changed their treatment plans. Future studies need to include more nonresponders to establish prediction models for treatment-resistant depression and thereby explore the different neuroimaging biomarkers between patients with different treatment outcomes. Fourth, although the significance level of our results was corrected for multiple comparisons using the FDR method, the effect sizes of subtype differences are relatively small. These findings suggest that there may be remaining heterogeneity within each subtype. Uncovering disease heterogeneity, especially in relation to clinical symptoms from the perspective of brain functional connectome, warrants further investigation. Fifth, an episode of MDD may be caused by numerous different factors, such as genetic liability, childhood adversity, and life stress (2,71,72). Several studies have identified genetic subtypes of MDD based on the heritability of single nucleotide polymorphisms (15,72). Additionally, neurobiological subtypes of MDD have been shown to exhibit different polygenic risk scores, expression of high-risk genetic profiles, and Child Abuse Trauma Scale scores (47,73). Future studies incorporating more comprehensive genetic and environmental data will provide valuable insight into the factors that lead to the different neurophysiological subtypes. Finally, we used 10-fold and leave-one-site-out cross-validation to validate the stability of the normative model and neurophysiological subtypes in our study and found good internal generalizability of our results. To maximize generalizability and replicability and reduce bias in model evaluation of our study, external validation in independent datasets from other populations and demographic groups is needed in future research.

ACKNOWLEDGMENTS AND DISCLOSURES

This work was supported by the SIT 2030-Major Projects (Grant No. 2022ZD0211500 [to MX]), National Natural Science Foundation of China (Grant No. 82071998 [to MX]; Grant No. 82021004 [to YH]; Grant Nos. 81920108019, 91649117, 81771344, and 81471251 [to SQ]), Beijing Nova Program (Grant No. Z191100001119023 [to MX]), Beijing United Imaging Research Institute of Intelligent Imaging Foundation (Grant No. CRIBJZD202102 [to MX]), Science and Technology Plan Project of Guangzhou (Grant No. 2018-1002-SF-0442 [to SQ]), Guangzhou Key Laboratory (Grant No. 09002344 [to SQ]), and Key R&D Program of Sichuan Province (Grant No. 2023YFS0076 [to TC]).

A previous version of this article was published as a preprint on bioRxiv: https://doi.org/10.1101/2023.02.13.528399.

The authors report no biomedical financial interests or potential conflicts of interest.

ARTICLE INFORMATION

From the State Key Laboratory of Cognitive Neuroscience and Learning, Beijing Normal University, Beijing, China (XS, JL, QM, YH, MX); Beijing Key Laboratory of Brain Imaging and Connectomics, Beijing Normal University, Beijing, China (XS, JL, QM, YH, MX); IDG/McGovern Institute for Brain Research, Beijing Normal University, Beijing, China (XS, JL, QM, YH, MX); School of Systems Science, Beijing Normal University, Beijing, China (XS, WW); Department of Psychiatry and National Clinical Research Center for Mental Disorders, The Second Xiangya Hospital of Central South University, Changsha, Hunan, China (JS, XL, QD, LZ, BL, LL); Mental Health Institute of Central South University, China National Technology Institute on Mental Disorders, Hunan Technology Institute of Psychiatry, Hunan Key Laboratory of Psychiatry and Mental Health, Hunan Medical Center for Mental Health, Changsha, Hunan, China (JS, XL, QD, LZ, BL, LL); Affiliated WuTaiShan Hospital of Medical College of Yangzhou University, Yangzhou Mental Health Centre, Yangzhou, China (JS); Affiliated Wuhan Mental Health Center, Huazhong University of Science and Technology, Wuhan, China (XL); Department of Psychiatry, Lanzhou University Second Hospital, Lanzhou, China (QD); Mental Health Education and Counseling Center, Shanghai University of Medicine and Health Sciences, Shanghai, China (LZ); Institute of Science and Technology for Brain-Inspired Intelligence, Fudan University, Shanghai, China (QM); Key Laboratory of Cognition and Personality (Southwest University), Ministry of Education, Chongqing, China (XW, DW, JQ); Department of Psychology, Southwest University, Chongqing, China (XW, DW, JQ); Department of Magnetic Resonance Imaging, The First Affiliated Hospital of Zhengzhou University, Zhengzhou, China (YC, JC); Shanghai Key Laboratory of Brain Functional Genomics (Ministry of Education), Affiliated Mental Health Center, School of Psychology and Cognitive

Science, East China Normal University, Shanghai, China (C-CH); Department of Radiology, The First Affiliated Hospital of Guangzhou University of Chinese Medicine, Guangzhou, China (YZ, SQ); Peking University Sixth Hospital, Peking University Institute of Mental Health, National Health Commission Key Laboratory of Mental Health (Peking University), National Clinical Research Center for Mental Disorders (Peking University Sixth Hospital), Peking University, Beijing, China (YW, TS); Huaxi Magnetic Resonance Research Center, Department of Radiology, West China Hospital, Sichuan University, Chengdu, China (TC, QG); Department of Psychiatry, First Affiliated Hospital of Kunming Medical University, Kunming, China (YC, XX); Research Unit of Psychoradiology, Chinese Academy of Medical Sciences, Chengdu, Sichuan, China (QG); Institute of Neuroscience, National Yang-Ming Chiao-Tung University, Taipei, Taiwan (C-PL); Department of Education and Research, Taipei City Hospital, Taipei, Taiwan (C-PL); Department of Psychiatry, The First Affiliated Hospital of China Medical University, Shenyang, China (YT, FW); Chongqing Key Laboratory of Neurobiology, Chongqing, China (PX); Department of Neurology, The First Affiliated Hospital of Chongqing Medical University, Chongqing, China (PX); and Chinese Institute for Brain Research, Beijing, China (YH).

DIDA-MDD Working Group includes Yong He, Lingjiang Li, Jingliang Cheng, Qiyong Gong, Ching-Po Lin, Jiang Qiu, Shijun Qiu, Tianmei Si, Yanqing Tang, Fei Wang, Peng Xie, Xiufeng Xu, and Mingrui Xia.

Address correspondence to Mingrui Xia, Ph.D., at mxia@bnu.edu.cn.

Received Mar 9, 2023; revised May 15, 2023; accepted May 29, 2023.

Supplementary material cited in this article is available online at https://doi.org/10.1016/j.biopsych.2023.05.021.

REFERENCES

1. World Health Organization (2017): Depression and Other Common Mental Disorders: Global Health Estimates. Geneva: World Health Organization.
2. Malhi GS, Mann JJ (2018): Depression. Lancet 392:2299–2312.
3. Kaufmann T, van der Meer D, Doan NT, Schwarz E, Lund MJ, Agartz I, *et al.* (2019): Common brain disorders are associated with heritable patterns of apparent aging of the brain. Nat Neurosci 22:1617–1623.
4. Marín O (2016): Developmental timing and critical windows for the treatment of psychiatric disorders. Nat Med 22:1229–1238.
5. van Loo HM, de Jonge P, Romeijn JW, Kessler RC, Schoevers RA (2012): Data-driven subtypes of major depressive disorder: A systematic review. BMC Med 10:156.
6. Harald B, Gordon P (2012): Meta-review of depressive subtyping models. J Affect Disord 139:126–140.
7. Maglanoc LA, Landrø NI, Jonassen R, Kaufmann T, Córdova-Palomera A, Hilland E, Westlye LT (2019): Data-driven clustering reveals a link between symptoms and functional brain connectivity in depression. Biol Psychiatry Cogn Neurosci Neuroimaging 4:16–26.
8. Kaiser RH, Andrews-Hanna JR, Wager TD, Pizzagalli DA (2015): Large-scale network dysfunction in major depressive disorder: A meta-analysis of resting-state functional connectivity. JAMA Psychiatry 72:603–611.
9. Fornito A, Zalesky A, Breakspear M (2015): The connectomics of brain disorders. Nat Rev Neurosci 16:159–172.
10. Gong Q, He Y (2015): Depression, neuroimaging and connectomics: A selective overview. Biol Psychiatry 77:223–235.
11. Xia M, Liu J, Mechelli A, Sun X, Ma Q, Wang X, *et al.* (2022): Connectome gradient dysfunction in major depression and its association with gene expression profiles and treatment outcomes. Mol Psychiatry 27:1384–1393.
12. Fox MD, Liu H, Pascual-Leone A (2013): Identification of reproducible individualized targets for treatment of depression with TMS based on intrinsic connectivity. Neuroimage 66:151–160.
13. Cash RFH, Weigand A, Zalesky A, Siddiqi SH, Downar J, Fitzgerald PB, Fox MD (2021): Using brain imaging to improve spatial targeting of transcranial magnetic stimulation for depression. Biol Psychiatry 90:689–700.
14. Sun X, Liu J, Ma Q, Duan J, Wang X, Xu Y, *et al.* (2021): Disrupted intersubject variability architecture in functional connectomes in schizophrenia. Schizophr Bull 47:837–848.
15. Beijers L, Wardenaar KJ, van Loo HM, Schoevers RA (2019): Data-driven biological subtypes of depression: Systematic review of biological approaches to depression subtyping. Mol Psychiatry 24:888–900.
16. Drysdale AT, Grosenick L, Downar J, Dunlop K, Mansouri F, Meng Y, *et al.* (2017): Resting-state connectivity biomarkers define neurophysiological subtypes of depression. Nat Med 23:28–38.
17. Liang S, Deng W, Li X, Greenshaw AJ, Wang Q, Li M, *et al.* (2020): Biotypes of major depressive disorder: Neuroimaging evidence from resting-state default mode network patterns. Neuroimage Clin 28:102514.
18. Wang X, Qin J, Zhu R, Zhang S, Tian S, Sun Y, *et al.* (2022): Predicting treatment selections for individuals with major depressive disorder according to functional connectivity subgroups. Brain Connect 12:699–710.
19. Wang Y, Tang S, Zhang L, Bu X, Lu L, Li H, *et al.* (2021): Data-driven clustering differentiates subtypes of major depressive disorder with distinct brain connectivity and symptom features. Br J Psychiatry 219:606–613.
20. Marquand AF, Rezek I, Buitelaar J, Beckmann CF (2016): Understanding heterogeneity in clinical cohorts using normative models: Beyond case-control studies. Biol Psychiatry 80:552–561.
21. Marquand AF, Kia SM, Zabihi M, Wolfers T, Buitelaar JK, Beckmann CF (2019): Conceptualizing mental disorders as deviations from normative functioning. Mol Psychiatry 24:1415–1424.
22. Marquand AF, Wolfers T, Mennes M, Buitelaar J, Beckmann CF (2016): Beyond lumping and splitting: A review of computational approaches for stratifying psychiatric disorders. Biol Psychiatry Cogn Neurosci Neuroimaging 1:433–447.
23. Cole TJ (2012): The development of growth references and growth charts. Ann Hum Biol 39:382–394.
24. Zabihi M, Oldehinkel M, Wolfers T, Frouin V, Goyard D, Loth E, *et al.* (2019): Dissecting the heterogeneous cortical anatomy of autism spectrum disorder using normative models. Biol Psychiatry Cogn Neurosci Neuroimaging 4:567–578.
25. Wolfers T, Beckmann CF, Hoogman M, Buitelaar JK, Franke B, Marquand AF (2020): Individual differences v. the average patient: Mapping the heterogeneity in ADHD using normative models. Psychol Med 50:314–323.
26. Wolfers T, Doan NT, Kaufmann T, Alnæs D, Moberget T, Agartz I, *et al.* (2018): Mapping the heterogeneous phenotype of schizophrenia and bipolar disorder using normative models. JAMA Psychiatry 75:1146–1155.
27. Shan X, Uddin LQ, Xiao J, He C, Ling Z, Li L, *et al.* (2022): Mapping the heterogeneous brain structural phenotype of autism spectrum disorder using the normative model. Biol Psychiatry 91:967–976.
28. Xia M, Si T, Sun X, Ma Q, Liu B, Wang L, *et al.* (2019): Reproducibility of functional brain alterations in major depressive disorder: Evidence from a multisite resting-state functional MRI study with 1,434 individuals. Neuroimage 189:700–714.
29. Shen X, Tokoglu F, Papademetris X, Constable RT (2013): Groupwise whole-brain parcellation from resting-state fMRI data for network node identification. Neuroimage 82:403–415.
30. Rasmussen CE, Williams CKI (2006): Gaussian Processes for Machine Learning. Cambridge: MIT Press.
31. Dimitrova R, Arulkumaran S, Carney O, Chew A, Falconer S, Ciarrusta J, *et al.* (2021): Phenotyping the preterm brain: Characterizing individual deviations from normative volumetric development in two large infant cohorts. Cereb Cortex 31:3665–3677.
32. Tomasi D, Volkow ND (2012): Aging and functional brain networks. Mol Psychiatry 17:549–558.
33. Wu K, Taki Y, Sato K, Hashizume H, Sassa Y, Takeuchi H, *et al.* (2013): Topological organization of functional brain networks in healthy children: Differences in relation to age, sex, and intelligence. PLoS One 8:e55347.
34. Cao M, Wang JH, Dai ZJ, Cao XY, Jiang LL, Fan FM, *et al.* (2014): Topological organization of the human brain functional connectome across the lifespan. Dev Cogn Neurosci 7:76–93.
35. Dai Z, Yan C, Li K, Wang Z, Wang J, Cao M, *et al.* (2015): Identifying and mapping connectivity patterns of brain network hubs in Alzheimer's disease. Cereb Cortex 25:3723–3742.

36. Filley CM, Cullum CM (1994): Attention and vigilance functions in normal aging. Appl Neuropsychol 1:29–32.
37. Sambataro F, Murty VP, Callicott JH, Tan HY, Das S, Weinberger DR, Mattay VS (2010): Age-related alterations in default mode network: Impact on working memory performance. Neurobiol Aging 31:839–852.
38. Feczko E, Miranda-Dominguez O, Marr M, Graham AM, Nigg JT, Fair DA (2019): The heterogeneity problem: Approaches to identify psychiatric subtypes. Trends Cogn Sci 23:584–601.
39. Feczko E, Fair DA (2020): Methods and challenges for assessing heterogeneity. Biol Psychiatry 88:9–17.
40. Yang Y, Zhu DM, Zhang C, Zhang Y, Wang C, Zhang B, *et al.* (2020): Brain structural and functional alterations specific to low sleep efficiency in major depressive disorder. Front Neurosci 14:50.
41. Zhang J, Wang J, Wu Q, Kuang W, Huang X, He Y, Gong Q (2011): Disrupted brain connectivity networks in drug-naive, first-episode major depressive disorder. Biol Psychiatry 70:334–342.
42. Wang L, Dai Z, Peng H, Tan L, Ding Y, He Z, *et al.* (2014): Overlapping and segregated resting-state functional connectivity in patients with major depressive disorder with and without childhood neglect. Hum Brain Mapp 35:1154–1166.
43. Wang L, Xia M, Li K, Zeng Y, Su Y, Dai W, *et al.* (2015): The effects of antidepressant treatment on resting-state functional brain networks in patients with major depressive disorder. Hum Brain Mapp 36:768–778.
44. Shi Y, Li J, Feng Z, Xie H, Duan J, Chen F, Yang H (2020): Abnormal functional connectivity strength in first-episode, drug-naive adult patients with major depressive disorder. Prog Neuropsychopharmacol Biol Psychiatry 97:109759.
45. Zhang Y, Wu W, Toll RT, Naparstek S, Maron-Katz A, Watts M, *et al.* (2021): Identification of psychiatric disorder subtypes from functional connectivity patterns in resting-state electroencephalography. Nat Biomed Eng 5:309–323.
46. Price RB, Gates K, Kraynak TE, Thase ME, Siegle GJ (2017): Data-driven subgroups in depression derived from directed functional connectivity paths at rest. Neuropsychopharmacology 42:2623–2632.
47. Chang M, Womer FY, Gong X, Chen X, Tang L, Feng R, *et al.* (2021): Identifying and validating subtypes within major psychiatric disorders based on frontal-posterior functional imbalance via deep learning. Mol Psychiatry 26:2991–3002.
48. Greene AS, Shen X, Noble S, Horien C, Hahn CA, Arora J, *et al.* (2022): Brain-phenotype models fail for individuals who defy sample stereotypes. Nature 609:109–118.
49. Dhamala E, Yeo BTT, Holmes AJ (2023): One size does not fit all: Methodological considerations for brain-based predictive modeling in psychiatry. Biol Psychiatry 93:717–728.
50. Auerbach RP, Pagliaccio D, Allison GO, Alqueza KL, Alonso MF (2021): Neural correlates associated with suicide and nonsuicidal self-injury in youth. Biol Psychiatry 89:119–133.
51. Jollant F, Lawrence NL, Olié E, Guillaume S, Courtet P (2011): The suicidal mind and brain: A review of neuropsychological and neuroimaging studies. World J Biol Psychiatry 12:319–339.
52. Zhang H, Chen Z, Jia Z, Gong Q (2014): Dysfunction of neural circuitry in depressive patients with suicidal behaviors: A review of structural and functional neuroimaging studies. Prog Neuropsychopharmacol Biol Psychiatry 53:61–66.
53. Chen Z, Xia M, Zhao Y, Kuang W, Jia Z, Gong Q (2021): Characteristics of intrinsic brain functional connectivity alterations in major depressive disorder patients with suicide behavior. J Magn Reson Imaging 54:1867–1875.
54. Elliott R, Dolan RJ, Frith CD (2000): Dissociable functions in the medial and lateral orbitofrontal cortex: Evidence from human neuroimaging studies. Cereb Cortex 10:308–317.
55. Morrison R, O'Connor RC (2008): A systematic review of the relationship between rumination and suicidality. Suicide Life Threat Behav 38:523–538.
56. First M, Spitzer R, Gibbon M, Williams J (1997): Structured Clinical Interview for DSM-IV Axis I Disorders. Washington, DC: American Psychiatric Publishing.
57. Höflich A, Michenthaler P, Kasper S, Lanzenberger R (2019): Circuit mechanisms of reward, anhedonia, and depression. Int J Neuropsychopharmacol 22:105–118.
58. Su YA, Si T (2022): Progress and challenges in research of the mechanisms of anhedonia in major depressive disorder. Gen Psychiatr 35:e100724.
59. Felger JC, Li Z, Haroon E, Woolwine BJ, Jung MY, Hu X, Miller AH (2016): Inflammation is associated with decreased functional connectivity within corticostriatal reward circuitry in depression. Mol Psychiatry 21:1358–1365.
60. Gabbay V, Ely BA, Li Q, Bangaru SD, Panzer AM, Alonso CM, *et al.* (2013): Striatum-based circuitry of adolescent depression and anhedonia. J Am Acad Child Adolesc Psychiatry 52:628–641.e13.
61. Geller WN, Liu K, Warren SL (2021): Specificity of anhedonic alterations in resting-state network connectivity and structure: A transdiagnostic approach. Psychiatry Res Neuroimaging 317:111349.
62. Guo CC, Hyett MP, Nguyen VT, Parker GB, Breakspear MJ (2016): Distinct neurobiological signatures of brain connectivity in depression subtypes during natural viewing of emotionally salient films. Psychol Med 46:1535–1545.
63. Zhang T, He K, Bai T, Lv H, Xie X, Nie J, *et al.* (2021): Altered neural activity in the reward-related circuit and executive control network associated with amelioration of anhedonia in major depressive disorder by electroconvulsive therapy. Prog Neuropsychopharmacol Biol Psychiatry 109:110193.
64. Zisook S, Rush AJ, Albala A, Alpert J, Balasubramani GK, Fava M, *et al.* (2004): Factors that differentiate early vs. later onset of major depression disorder. Psychiatry Res 129:127–140.
65. Cui L, Wang Y, Cao L, Wu Z, Peng D, Chen J, *et al.* (2023): Age of onset for major depressive disorder and its association with symptomatology. J Affect Disord 320:682–690.
66. Klein DN, Schatzberg AF, McCullough JP, Dowling F, Goodman D, Howland RH, *et al.* (1999): Age of onset in chronic major depression: Relation to demographic and clinical variables, family history, and treatment response. J Affect Disord 55:149–157.
67. Gournellis R, Oulis P, Rizos E, Chourdaki E, Gouzaris A, Lykouras L (2011): Clinical correlates of age of onset in psychotic depression. Arch Gerontol Geriatr 52:94–98.
68. Korgaonkar MS, Goldstein-Piekarski AN, Fornito A, Williams LM (2020): Intrinsic connectomes are a predictive biomarker of remission in major depressive disorder. Mol Psychiatry 25:1537–1549.
69. Chin Fatt CR, Jha MK, Cooper CM, Fonzo G, South C, Grannemann B, *et al.* (2020): Effect of intrinsic patterns of functional brain connectivity in moderating antidepressant treatment response in major depression. Am J Psychiatry 177:143–154.
70. Dichter GS, Gibbs D, Smoski MJ (2015): A systematic review of relations between resting-state functional-MRI and treatment response in major depressive disorder. J Affect Disord 172:8–17.
71. Flint J, Kendler KS (2014): The genetics of major depression. Neuron 81:484–503.
72. Nguyen TD, Harder A, Xiong Y, Kowalec K, Hägg S, Cai N, *et al.* (2022): Genetic heterogeneity and subtypes of major depression. Mol Psychiatry 27:1667–1675.
73. Tokuda T, Yoshimoto J, Shimizu Y, Okada G, Takamura M, Okamoto Y, *et al.* (2018): Identification of depression subtypes and relevant brain regions using a data-driven approach. Sci Rep 8:14082.